The Canadian Mineralogist
Vol. 47, pp. 263-274 (2009)
DOI: 10.3749/canmin.47.2.263

THE CRYSTAL CHEMISTRY OF THE KORNERUPINE–PRISMATINE SERIES. II. THE ROLE OF HYDROGEN

MARK A. COOPER AND FRANK C. HAWTHORNE[§]

Department of Geological Sciences, University of Manitoba, Winnipeg, Manitoba R3T 2N2, Canada

EDWARD S. GREW

Department of Earth Sciences, University of Maine, Orono, Maine 04469, U.S.A.

GEORGE R. ROSSMAN

Division of Geological and Planetary Sciences, California Institute of Technology, Pasadena, California 91125, U.S.A.

ABSTRACT

The H contents of a suite of well-characterized samples of kornerupine–prismatine minerals, (□,Mg,Fe) (Al,Mg,Fe)$_9$ (Si,Al,B)$_5$ O$_{21}$ (OH,F), have been measured by KFT (Karl Fischer Titration) and HLE (Hydrogen-Line Extraction). The KFT results show (OH + F) < 1.0 *apfu* (atoms per formula unit); the deviation from 1.0 (OH + F) *apfu* is negatively correlated with the Fe content of kornerupine, whereas the HLE results show (OH + F) ≈ 1.0 *apfu*. Crystal-chemical considerations suggest that the HLE results are correct. The anomalously low KFT results are due to incomplete breakdown of the sample and only partial release of the constituent H. Detailed examination of the electron density around the O(10) (= OH) site in several crystals of kornerupine reveal two distinct *H* sites, *H*(1) and *H*(2); the *H*(1) site occurs on the (001) mirror plane, and the *H*(2) site occurs off the (001) mirror plane. The H atom is usually disordered off the (001) mirror plane (at z = ¼) at the *H*(2) site. The latter is only ~1.1 Å from the *X* site, and hence mutual occupancy of locally adjacent *H*(2) and *X* sites is not possible; this constraint gives the maximum possible occupancy of the *X* site as (1 + F)/2 *apfu*. Where H occupies the *H*(1) site on the (001) mirror plane, both adjacent *X* sites must be locally vacant. Polarized infrared spectra in the principal (OH)-stretching region show fine structure that can be assigned to specific short-range arrangements of cations around the O(10) [≡ (OH), F] site involving occupancy of the *X* site by divalent cations or vacancies, adjacent *T*(1) sites by Si–Si or Si–Al, adjacent *M*(1) sites by Mg or Fe^{2+}, and occupancy of the *H*(1) or *H*(2) sites by H or □.

Keywords: kornerupine, H_2O, electron density, chemical composition, polarized infrared spectra, short-range order.

SOMMAIRE

La teneur en H d'une série d'échantillons de kornérupine–prismatine bien caractérisés, (□,Mg,Fe) (Al,Mg,Fe)$_9$ (Si,Al,B)$_5$ O$_{21}$ (OH,F), a été mesurée par titration Karl Fischer (KFT) et par extraction complète de l'hydrogène (HLE). Selon la méthode KFT, la teneur en (OH + F) est inférieure à 1.0 *apfu* (atomes par formule unitaire); l'écart de 1.0 (OH + F) *apfu* montre une corrélation négative avec la teneur en Fe de la kornérupine, tandis que les résultats HLE montrent (OH + F) à peu près égal à 1.0 *apfu*. Les considérations cristallochimiques font penser que les résultats HLE sont fiables. Les valeurs anormalement basses obtenues par KFT seraient dues à la décomposition incomplète des échantillons et à la libération de seulement une partie de l'hydrogène. Un examen détaillé de la densité des électrons autour du site O(10) (= OH) dans plusieurs échantillons de kornérupine révèle deux sites *H* distincts, *H*(1) et *H*(2); le site *H*(1) est situé sur le plan miroir (001), tandis que le site *H*(2) ne l'est pas. L'atome H est généralement désordonné et déplacé par rapport au plan miroir (001), au site *H*(2) à z = ¼. Ce site se trouve seulement ~1.1 Å du site *X*, et donc l'occupation simultanée de sites *H*(2) et *X* localement adjacents est impossible; cette contrainte mène au taux d'occupation maximum du site *X*, (1 + F)/2 *apfu*. Dans les cas où H occupe le site *H*(1) sur le plan miroir (001), les deux sites *X* adjacents doivent être localement vacants. Les spectres polarisés dans l'infrarouge dans la région principale d'étirement (OH) montre une structure fine que l'on peut attribuer à des arrangement spécifiques à courte échelle autour du site O(10) [≡ (OH), F] impliquant un taux d'occupation du site *X* par des cations bivalents ou des lacunes, les sites *T*(1) adjacents par Si–Si ou Si–Al, les sites *M*(1) adjacents par Mg ou Fe^{2+}, et l'occupation des sites *H*(1) ou *H*(2) par H ou □.

(Traduit par la Rédaction)

Mots-clés: kornérupine, H_2O, densité des électrons, composition chimique, spectres dans l'infrarouge polarisés, mise en ordre à courte échelle.

§ *E-mail address*: frank_hawthorne@umanitoba.ca

Introduction

Understanding the behavior of light lithophile elements in a mineral is crucial to understanding the crystal chemistry of that mineral (Hawthorne 1995), yet these elements can be fairly intractable from an analytical viewpoint. Chemical analysis of kornerupine and prismatine (Grew 1996, Ottolini *et al.* 2002) shows a range of H_2O content. Previous structural studies (Moore & Bennett 1968, Moore & Araki 1979, Finger & Hazen 1981, Moore *et al.* 1989, Klaska & Grew 1991) have suggested that the O(10) anion site is occupied predominantly to completely by (OH). Chemical analyses also show a range of F content, and (presumably) there is (OH) ↔ F diadochy. However, the key point is whether the O(10) site is completely occupied by monovalent anions [*i.e.*, (OH) + F = 1.0 *apfu*, atoms per formula unit]. There are two important issues here: (1) if (OH) + F ≠ 1.0 *apfu*, then the anion species at O(10) must be involved in heterovalent substitutions in the kornerupine–prismatine structure, and the H_2O content in kornerupine–prismatine must be measured in order to calculate the chemical formula; (2) if (OH) + F is equal to 1.0 *apfu*, then this constraint can be incorporated into the normalization procedure to calculate the chemical formula from the chemical composition. Thus resolution of the role of H in the structure of kornerupine–prismatine is essential if we are to understand structural and chemical variations in these minerals.

Experimental

Samples for this work were taken from the sample set of Cooper *et al.* (2009). The numbers of samples used for the different experimental techniques was limited severely by the amount of homogeneous clean material available for analytical work.

Chemical analysis

The H content was measured by two different methods: (1) Karl Fischer titration (KFT); (2) H-line extraction (HLE).

KFT: The sample (25–50 mg of finely divided powder) was heated in a fused-silica tube at a nominal temperature of 900°C in a furnace for ~15 minutes. A stream of N_2 gas carried the evolved gases into a cell containing two electrodes and a pyridine–methanol solution that contained iodine and sulfur dioxide as principal ingredients. Iodide ions are generated electrolytically at the anode, and react with any H_2O present according to the following scheme: $I_2 + SO_2 + H_2O \rightarrow 2HI + SO_3$. The iodide generated is in direct proportion to the electric current according to Faraday's Law: $2I^- - 2e \rightarrow I_2$. Thus the amount of H_2O present is determined by the quantity of current required for electrolysis.

HLE: Samples of ~50 mg of fine-grained powder were wrapped in molybdenum foil and placed in a platinum crucible, which was then suspended inside a fused-silica extraction vessel (Kyser & O'Neil 1984). The vessel and its contents were outgassed in a vacuum at 150°C for 12 h to remove surface-adsorbed water. The sample was then inductively heated at 1400°C for 20 minutes, and the gases were collected in a trap held at –196°C. Nearly all of the hydrogen was released in the form of water, but minuscule quantities of hydrocarbons or molecular hydrogen released or produced during this treatment were oxidized over CuO at 500°C to form H_2O and CO_2, which were also collected in the trap. The accumulated water representing the total amount of hydrogen in the samples was separated from the other gases by differential freezing techniques. The water was reacted with uranium at 750°C to produce H_2 and collected on charcoal at –196°C. The volume of the H_2 was measured manometrically.

Infrared spectroscopy

Single crystals were oriented by X-ray precession photography, and then cut such that the plane of the slice is orthogonal to a crystallographic axis. For each sample of kornerupine–prismatine, two such slabs oriented orthogonal to two different crystallographic axes were ground to a thickness between 30 and 50 μm and then polished on both sides. Spectra were obtained on a Nicolet 60SX FTIR instrument with a LN_2-cooled MCT–A detector and a CaF_2 beamsplitter. Slabs of crystal were aligned optically in polarized light prior to measurement, and the resulting spectra were normalized to a standard thickness of 100 μm.

Results

Determination of H_2O content

The values from the two different methods are listed in Table 1, and are compared with the values calculated from the relation OH = 1 – F *apfu* in Figure 1. There is considerable disparity between the two sets of experimental results: (1) the KFT results are less than the stoichiometric values; (2) the HLE results are approximately equal to the stoichiometric values. Figure 2 shows the variation in H_2O (experimental) – H_2O (stoichiometric) as a function of ^{T}FeO content (^{T}FeO indicates total Fe expressed as FeO, values from Cooper *et al.* 2009); it is apparent from this figure that the deviations of the KFT data from stoichiometric values vary systematically as a function of ^{T}FeO content.

KFT values: These values are systematically lower than the stoichiometric values; the deviations are greatest for the low-Fe samples, and decrease with increasing ^{T}FeO content. In the KFT method, the sample is heated in a fused-silica boat in a muffle furnace to a nominal temperature of 900°C. The sample breaks down, releasing H_2O, which then reacts with the iodide generated at the anode, as outlined above. Accurate analysis

of the sample requires that the sample completely break down and release all the H in the structure. In most (Mg,Fe) solid-solutions, the Mg end-member is much more refractory than the Fe end-member; there is no experimental evidence of the effect of Fe on the stability of kornerupine–prismatine, but it seems a reasonable deduction that Fe-poor crystals are more refractory than Fe-rich crystals. In the heating cycle of the KFT procedure, it seems that kornerupine–prismatine is not completely breaking down and releasing all of the H in the structure. If this is the case, one would expect the more refractory low-Fe kornerupine samples to be more resistant to breakdown and hence release less H than the high-Fe kornerupine samples.

HLE values: These values cluster around the stoichiometric values (Fig. 2). The estimated error is ± 0.1 wt.% H_2O, and none of the data deviate from the ideal value by more than twice the error. The HLE method is similar to the KFT method in that the H is released from the structure by heating the sample. However, in the HLE method, the sample is heated to 1400°C, compared to 900°C for the KFT method. It seems reasonable to conclude that 1400°C exceeds the stability of both low-Fe and high-Fe kornerupine, and hence all H is released from the kornerupine samples during heating, irrespective of Fe content.

The H_2O Content of Kornerupine–Prismatine: Experimental Determinations

The results of the two different methods of H_2O analysis used here give us significantly different deter-

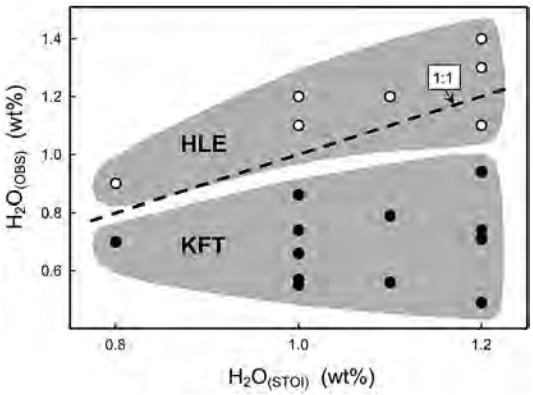

FIG. 1. Experimentally determined H_2O values in kornerupine–prismatine as a function of stoichiometrically calculated H_2O values; black circles: KFT data; open circles: HLE data; the dashed line shows the 1:1 relation.

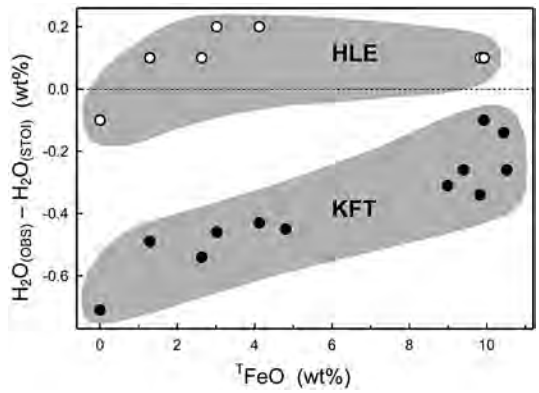

FIG. 2. The difference H_2O (experimental) – H_2O (stoichiometric) in kornerupine–prismatine as a function of ^{T}FeO content (total Fe expressed as FeO); legend as in Figure 1.

TABLE 1. KORNERUPINE–PRISMATINE: H_2O CONTENTS (wt.%) MEASURED BY VARIOUS METHODS

	KFT	HLE	STOI*	^{T}FeO**	Original #	Source locality
K2	0.74	1.4	1.2	3.02	133771	Bjørnesund, West Greenland
K5*	0.57(5)	1.2	1.0	4.13	–	Elahera, Sri Lanka
K6	0.66	1.1	1.0	9.83	134E	Aldan Shield, Yakutia, Russia
K8	0.94	–	1.2	9.40	3053B	Ponakkadu, India
K9	0.55	–	1.0	4.80	141255	Madagascar
K10	0.79	–	1.1	8.99	24518	Lac Sainte-Marie, Quebec, Canada
K15	0.74	–	1.0	10.52	5032	Baldwin Locality, Harts Range, Australia
K17	0.86	–	1.0	10.44	24752	Harts Range, Australia
K22	0.71	1.3	1.2	1.29	8497	Sinyoni Claims, Limpopo, Zimbabwe
K23	0.49	1.1	1.2	0.00	BM1978,467	Kwale, Kenya
K25	0.70	0.9	0.8	9.93	8812903	Larsemann Hills, East Antarctica
K32	0.56	1.2	1.1	2.63	–	Sri Lanka

* Calculated from the relation OH = 1 – F (*apfu*); ** Fe(total) as FeO, expressed in wt.%. * Based on eight measurements. KFT: Karl Fischer titration; HLE: hydrogen-line extraction; STOI: stoichiometry. Original #: original number of the sample.

minations of the H content of kornerupine–prismatine. However, the above discussion suggests that there are systematic errors in the KFT results, errors that are not unexpected when the details of the experimental methods and the chemical and physical properties of the samples are considered. The fact that the KFT results show a positive correlation with ^{T}FeO content, whereas the HLE results do not, allows the effect to be recognized.

For the purposes of crystal chemistry, we discard the results of the KFT experiments. Are the HLE results accurate? According to the above discussion, the HLE results should be free of the problem of incomplete release of hydrogen that seems to plague the KFT results, and hence there seems to be no physical problem with the HLE procedure. Furthermore, the experimental values are close to those derived stoichiometrically (Fig. 2). This agreement tends to validate *both* issues: (1) the HLE values are accurate; (2) the relation OH + F = 1 *apfu* in kornerupine–prismatine is correct. This is a reasonable conclusion from the results, but it should be accompanied by two caveats:

(1) the HLE results deviate from the stoichiometric values sufficiently to allow deviations from the stoichiometric relation of up to ~10% (except for K5, which shows a deviation of 20%). These small discrepancies may be due to random error in the determinations of both F (by electron-microprobe analysis) and H (by HLE), as the precision in the case of the former method is of the order of 10%.

(2) We only measured seven samples by HLE; it is possible that we analyzed samples only where OH + F ≈ 1 *apfu*, whereas there are other samples in which OH + F ≠ 1 *apfu*. Thus the conclusion that OH + F = 1 *apfu* in kornerupine–prismatine is only provisional from these analytical results, as the diffraction results discussed below also impact on this conclusion.

Experimental Determination of F in Kornerupine

In some of the arguments given above, we examine the quantity OH + F *apfu* in order to evaluate the accuracy of various sets of analytical results for the analysis of H_2O. In these arguments, we assume implicitly that there is no systematic error in the determination of F, *i.e.*, that the F values are accurate and have adequate precision. We can examine this assumption, as we have determined the F content of the kornerupine samples examined here by two different methods: (1) electron-microprobe analysis, and (2) site-scattering refinement (Cooper *et al.* 2009). As the physical bases of these techniques are completely different, they cannot have correlated error. Hence the results may be used to test the accuracy of the results. Figure 3 compares the two sets of results for F in kornerupine; the data scatter about a 1:1 line, indicating that both methods are accurate. Moreover, only two data points deviate from the 1:1 line by more than 2.7σ (the 99% confidence limit), suggesting that the precision of the electron-microprobe values is reasonably accurate.

Electron Density Around the O(10) Site

At the final stages of crystal-structure refinement (Cooper *et al.* 2009), the residual electron-density was examined in detail. The only significant density remaining in difference-Fourier maps is invariably less than one electron, and invariably occurs on the (100) plane at $x = 0$. For all refinements, the density was contoured, and the different patterns of contours are shown in Figure 4. There are three different types of pattern of residual electron-density: (1) the density maxima lie on the (001) mirror at $z = ¼$ [*i.e.*, *H*(1); K21]; (2) the density maxima are disordered off the (001) mirror at $z = ¼$ [*i.e.*, *H*(2); K22, K28, K38]; (3) electron-density maxima occur at both *H*(1) and *H*(2) sites (*e.g.*, K18). The black arrows in Figure 4 show a progression from a strong *H*(1) presence to a strong *H*(2) presence with transitional signatures in between. The majority of the samples show contours that are similar to pattern (2), and *H*(2) is usually the more prominent site.

Hydrogen Bonding in Kornerupine–Prismatine

The O(10) site is occupied by (OH) and bridges two *M*(1) octahedra, and the H atom of the (OH) group hydrogen-bonds to the O(9) site that bridges the two *T*(1) tetrahedra (Fig. 5). The H atom is constrained to the (001) mirror plane where it occupies the *H*(1) site, and is displaced off the (001) mirror plane where it occupies the *H*(2) site (Figs. 4, 5). Where the *H*(1) site is occupied, the H atom hydrogen bonds to the O(9) anion

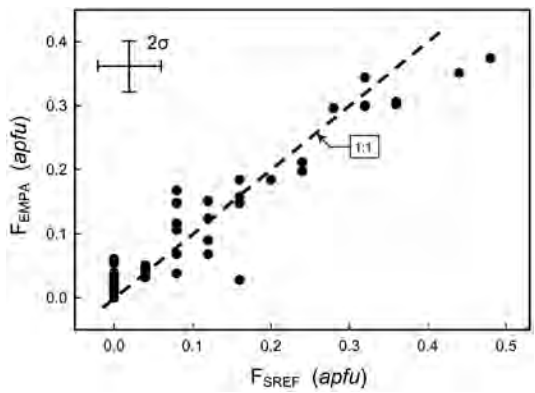

FIG. 3. Comparison of F determined by electron-microprobe analysis (EMPA) and site-scattering refinement (SREF) in 47 crystals of kornerupine–prismatine; the dashed line has a slope of unity.

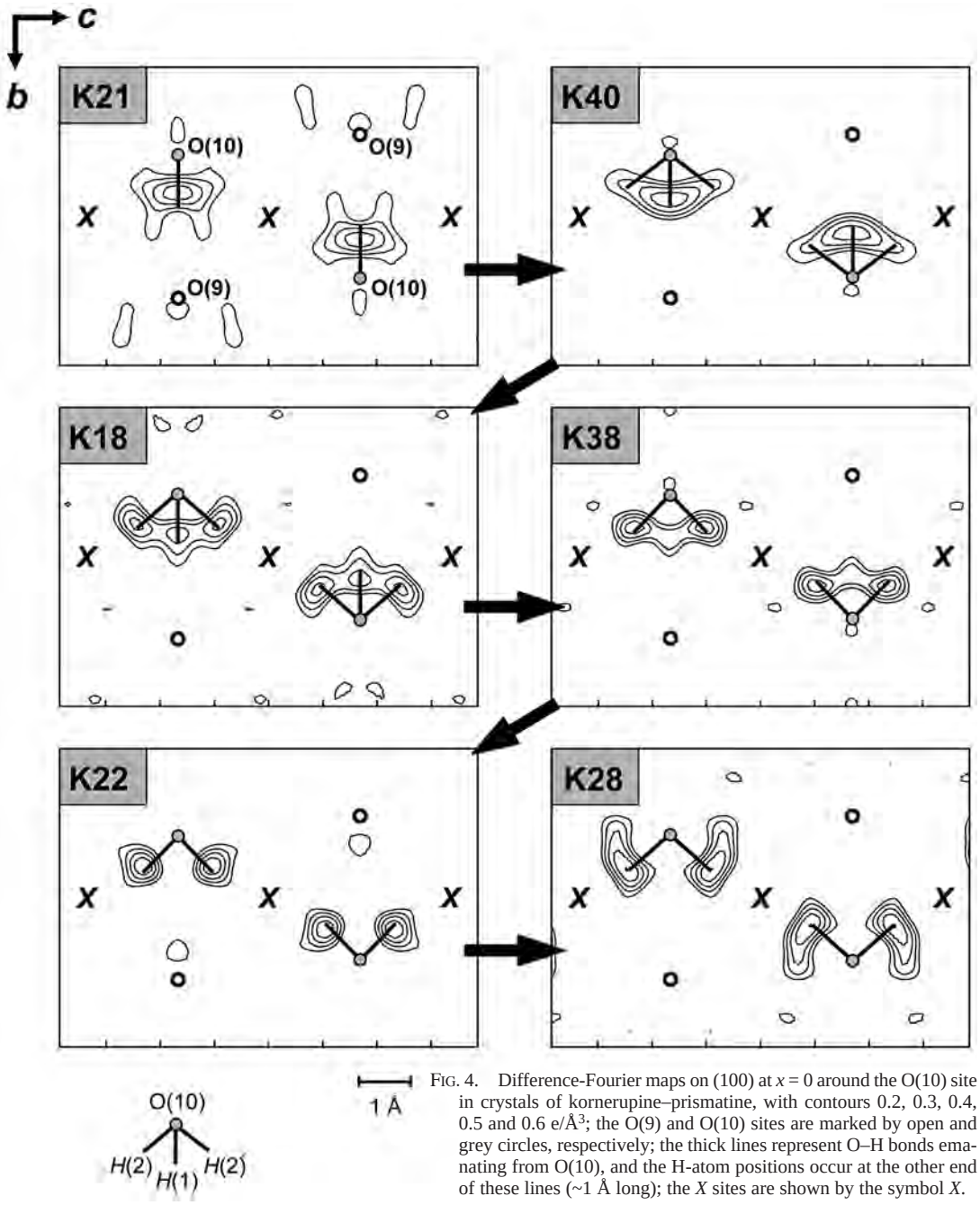

FIG. 4. Difference-Fourier maps on (100) at $x = 0$ around the O(10) site in crystals of kornerupine–prismatine, with contours 0.2, 0.3, 0.4, 0.5 and 0.6 e/Å^3; the O(9) and O(10) sites are marked by open and grey circles, respectively; the thick lines represent O–H bonds emanating from O(10), and the H-atom positions occur at the other end of these lines (~1 Å long); the *X* sites are shown by the symbol *X*.

of the adjacent sheet in the *b* direction (Fig. 5). Where the *H*(2) site is occupied, the H atom hydrogen bonds to the O(9) anion either in the *c* direction [O(9)^c] or to the O(9) anion in the adjacent sheet in the *b* direction [O(9)^b] (Fig. 5) (Klaska & Grew 1991). For crystals that show a high occupancy of *H*(2), the relations 2.52 < *H*(2)...O(9)^c < 2.89 Å and 2.21 < *H*(2)...O(9)^b < 2.66 Å, and 113 < O(10)–*H*(2)...O(9)^c < 147° and 87 < O(10)–*H*(2)...O(9)^b < 117° apply, where O(9)^c and O(9)^b denote the O(9) anions adjacent to *H*(2) in the

c and *b* directions, respectively (Fig. 6). It is apparent from the two extreme configurations in Figure 6 that, in some cases, O(9)^b would be favored over O(9)^c as the likely acceptor, and *vice versa*. In some of the difference-Fourier maps, the electron density associated with *H*(2) is smeared, indicating positional disorder, and hydrogen bonding is likely directed to both O(9)^b and O(9)^c within different regions of the crystal (*i.e.*, K28, Fig. 4).

Short-Range Order Involving the *H* and *X* Sites

Where an *H*(1) site is occupied in a local arrangement, the two adjacent *X* sites must be vacant because of the close distance between *H*(1) and *X* (Cooper *et al.* 2009); this is quite straightforward. However, the situation for occupancy of the *H*(2) and *X* sites is somewhat more complicated. The two different possible configurations for the hydrogen bonding involving *H*(2) do not affect the issue of short-range order, as the same atoms are involved in both configurations. The *H*(2) site is ~1.1 Å from the *X* site, and the mutual local occupancy of *X* and *H*(2) sites is therefore not possible. Both the H content at *H*(2) [F + OH = 1] and *H*(2) ordering can limit the occupancy of the *X* site. Two end-member schemes of order are shown in Figures 7a and 7b for OH = 1 *apfu*. If the OH bond is progressively staggered along *c*, then each succeeding *X* site is forced to be vacant (Fig. 7a) and the occupancy of *X* is zero. If successive pairs of OH bonds are directed toward each other along *c*, then only every other *X* site is forced to be vacant (Fig. 7b), and the occupancy of *X* can reach 0.5 *apfu*. The *X* site occupancies in this study range from 0.18 to 0.41 *apfu* (Cooper *et al.* 2009) and fall between the extremes of 0.0 and 0.5 *apfu*, suggested by Figures 7a and 7b.

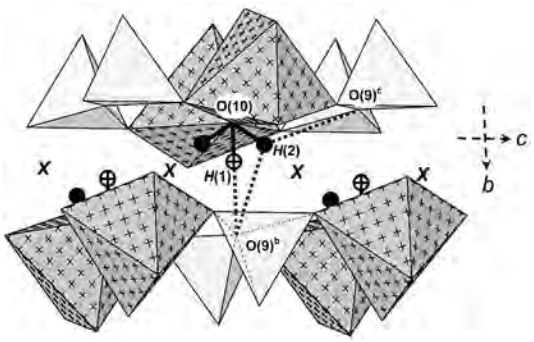

FIG. 5. The structural arrangement around the O(9) and O(10) sites in kornerupine–prismatine; circle with cross: H(1) site; black circle: H(2) site; *X* sites are shown by the symbol *X*; dark- grey-shaded octahedra with cross pattern: *M*(1) polyhedra; light-grey-shaded tetrahedra: *T*(1) polyhedra; hydrogen bonds are shown as dashed lines.

Also shown in Figures 7c and 7d are two possible schemes of order involving ⅓ and ½ H_2O *pfu*, respectively. Geometrically, these arrangements allow for up to ⅓ and ¼ occupancy of the *X* site. The *H*(2)–O(10)–*H*(2)' angles for K18, K38, K22 and K28 range from 102 to 116° and are acceptable angles for an H_2O group. The greatest difficulty in placing H_2O at the O(10) site is related to the details regarding a plausible H-bonding scheme (see next section). Although the local geometry seems reasonable for an H_2O group, the lack of suitable H-bond acceptors provides compelling evidence against H_2O substitution at O(10).

The Effect of F on the Maximum Occupancy of the *X* Site

Where the O(10) site is occupied by F, the short-range constraints of H on the occupancy of the *X* site are not present. The situation for maximum possible occupancy of O(10) by F and *X* by a cation is shown in Figure 8a. There are no steric restrictions on occupancy, and both O(10) and *X* can be fully occupied. Contrast this situation with occupancy of O(10) by (OH). Where the *H*(1) site is occupied (Fig. 8a), adjacent *X* sites must be vacant. Where the *H*(2) site is occupied (Fig. 8b), one adjacent *X* site must be vacant and the other adjacent *X* site may be occupied. Thus we may write a constraint on the maximum possible occupancy of the *X* site in terms of the occupancy of the O(10) site. For local arrangements (a), (b) and (c) (Fig. 8), the maximum occupancies of the *X* site are 1, 0 and 0.5, respectively. For a crystal made up of these three local arrangements, the occupancy of the *X* site is F [from arrangement (a)] + □ [from arrangement (b)] + (OH)/2 [from arrangement (c)]. The maximum occupancy of the *X* site may thus be written as F + (OH)/2 = F + (1 – F)/2 = (1 + F)/2.

Bond-Valence Considerations

Collectively, previous structural work on kornerupine–prismatine has resulted in proposals that the H content is variable from 0.0 to 1.x *apfu*. Thus the O(10) site should be occupied by O^{2-}, OH, F and H_2O. If this is true, it would require very different *local* (*i.e.*, short-range) cation arrangements about the O(10) site in order to satisfy the incident-bond-valence requirements for each of the constituent anion species.

The O(10) site occurs at the intersection of two mirror planes (‖ 100 and 001) at $x = 0$, $z = ¼$, and is adjacent to two *M*(1) sites and two *X* sites (Fig. 5). The *M*(1) site is completely occupied by divalent cations, whereas the *X* site is occupied by divalent cations (excluding negligible Na) and □ (vacancy). Hence there are three possible local arrangements of cations about the O(10) site; these are shown in Figure 9, together with the resulting incident bond-valences. Arrangement (1), with both *X* sites occupied (Fig. 9a), produces an incident bond-valence sum of 1⅓ *vu*. This

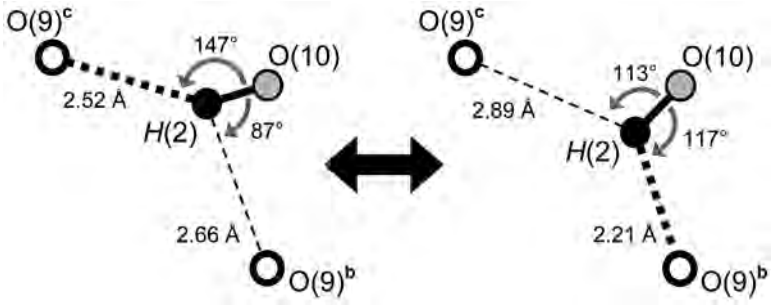

FIG. 6. Observed geometrical extremes for hydrogen bonding involving *H*(2) and alternate O(9) acceptors, along *c* [O(9)^c] and along *b* [O(9)^b]. Legend as in Figures 4 and 5.

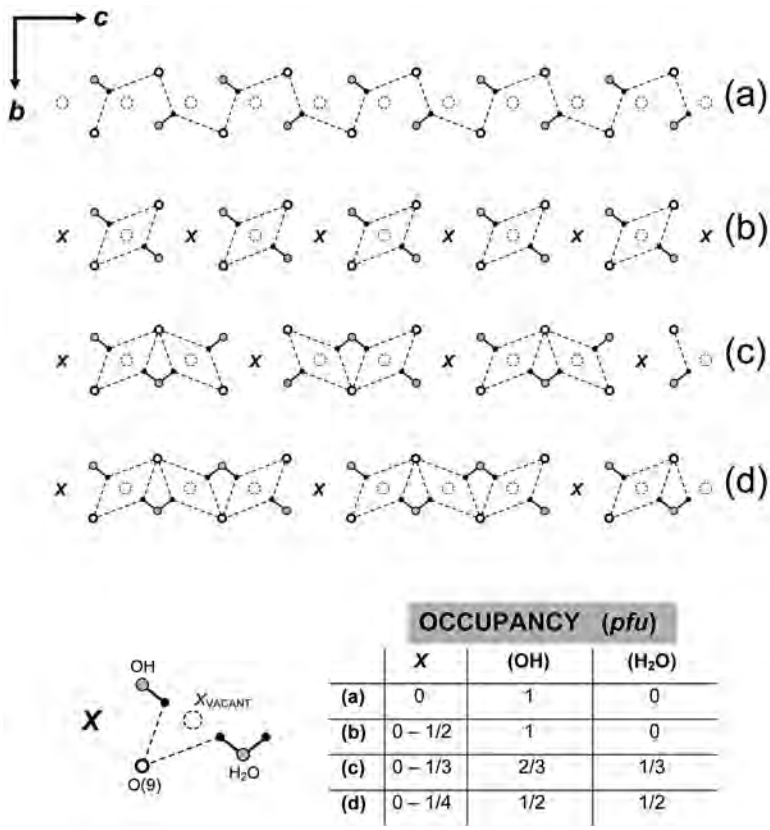

	OCCUPANCY (*pfu*)		
	X	(OH)	(H_2O)
(a)	0	1	0
(b)	0 – 1/2	1	0
(c)	0 – 1/3	2/3	1/3
(d)	0 – 1/4	1/2	1/2

FIG. 7. Schemes of local order involving H at the *H*(2) site and vacancies at the adjacent *X* sites; solid lines indicate O(donor)–H bonds; broken lines indicate H–O (acceptor) bonds. Legend as in Figures 4 and 5; empty dashed circles are vacant *X* sites. The amounts of *X* cation, (OH) and (H_2O) for the different arrangements are shown at the bottom right of the figure.

is the maximum incident bond-valence possible at the O(10) site (excluding any contribution from adjacent atoms of hydrogen); hence O^{2-} cannot occur at the O(10) site, as its incident bond-valence requirements cannot be satisfied. The *H*(2) and *X* sites are only ~1.1 Å apart, and local occupancy of both sites is not possible. Hence with two adjacent *X* sites occupied by (Mg,Fe^{2+}), the adjacent *H*(2) site cannot be occupied, and (OH) cannot occur at O(10). As O^{2-} cannot occur at O(10) and (OH) cannot occur at O(10) if both adjacent *X* sites are occupied, we may conclude that occupancy of adjacent *X* sites [*i.e.*, arrangement (1), Fig. 9a] is impossible; *this constraint imposes a maximum limit of 0.5 apfu on the occupancy of the X site in F-free kornerupine–prismatine.*

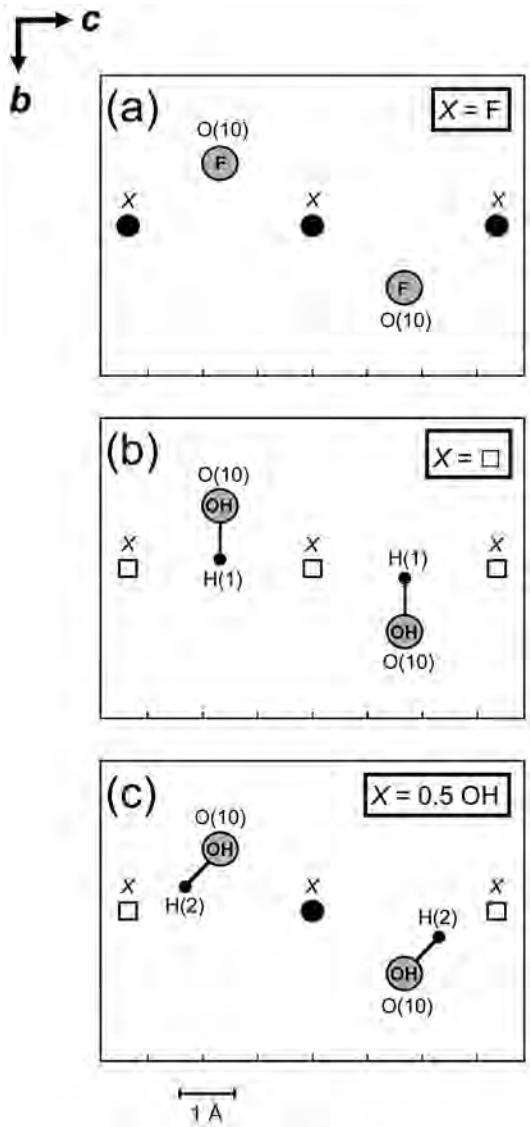

FIG. 8. Schemes of local order involving F and (OH) at O(10) and cation (•) and vacancies (□) at the *X* sites.

Arrangement (2), with one *X* site occupied (Fig. 9b), produces an incident-bond-valence sum at O(10) of 1.0 *vu*. The bond-valence requirements at the O(10) site may here be satisfied in two ways: (i) occurrence of F at O(10); (ii) occupancy of the adjacent *H*(2) site by a H atom. The fact that one of the two adjacent *X* sites is vacant also allows room for the *H*(2) site to be occupied.

Arrangement (3), with both *X* sites vacant (Fig. 9c), produces an incident-bond-valence sum of ⅔ *vu and* allows room for the occurrence of H atoms at both of the *H*(2) sites adjacent to O(10). In general, can an O-atom receive ~⅔ *vu* from adjacent cations and also bond to two H atoms? The answer is yes: kieserite, $Mg(SO_4)(H_2O)$, contains corner-sharing [$MgO_4(H_2O)$] chains in which (H_2O) bridges adjacent octahedra in the chain (Hawthorne *et al.* 1987). However, this type of arrangement requires very strong (~⅓ *vu*) H-bonds to other anions in the structure in order to satisfy the local bond-valence requirements around each H atom. In kornerupine, there are no suitable acceptors for such strong H-bonds. This problem is further exacerbated when the local arrangement is inspected (Figs. 7c, 7d, 9c): one third (Fig. 7c) or one half (Fig. 7d) of the O(9) sites would have to accept multiple H-bonds, in turn causing a significant excess of incident bond-valence at O(9). Thus the lack of suitable H-bond acceptors prevents the occurrence of (H_2O) at the O(10) site. The bond-valence requirements at the O(10) site for arrangement (3) may be satisfied in the same manner as for arrangement (2) [*i.e.*, a single *H*(2) site occupied or F at O(10)], with a concomitant shortening of the O(10)–*H*(2) or O(10)–*M*(1) distances (or both). To summarize, neither (H_2O) nor O^{2-} can occur at the O(10) site in minerals of the kornerupine–prismatine series.

INFRARED SPECTRA

The lack of any band at approximately 1630 cm^{-1} confirms our earlier conclusion that there are no (H_2O) groups in kornerupine; all H is present as (OH).

Polarization behavior

Inspection of the spectra in Figures 10 and 11 shows that there are no absorption bands in the spectra with E || *a*. This observation immediately constrains the O–H bond to lie in the (100) plane, in accord with the O(10) and *H* sites lying on the mirror plane at $x = 0$.

Bands A and B show absorption in both E || *b* and E || *c* spectra, whereas bands C, D and E show absorption only in one of the E || *b* or E || *c* spectra (Figs. 10, 11, Table 2). If the H atom occupies the Wyckoff position 4*c*

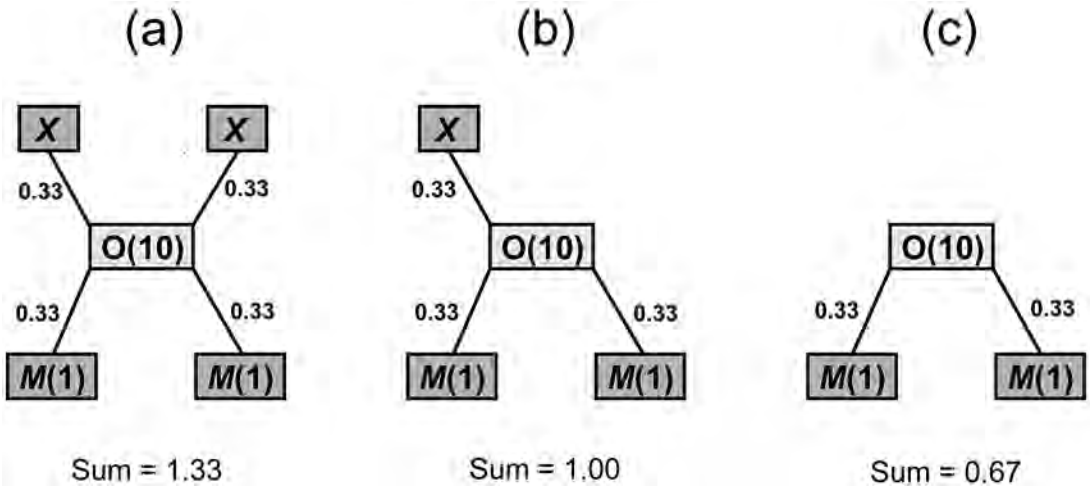

FIG. 9. Three possible local arrangements of cations about the O(10) site, together with the resulting bond-valence arrangements.

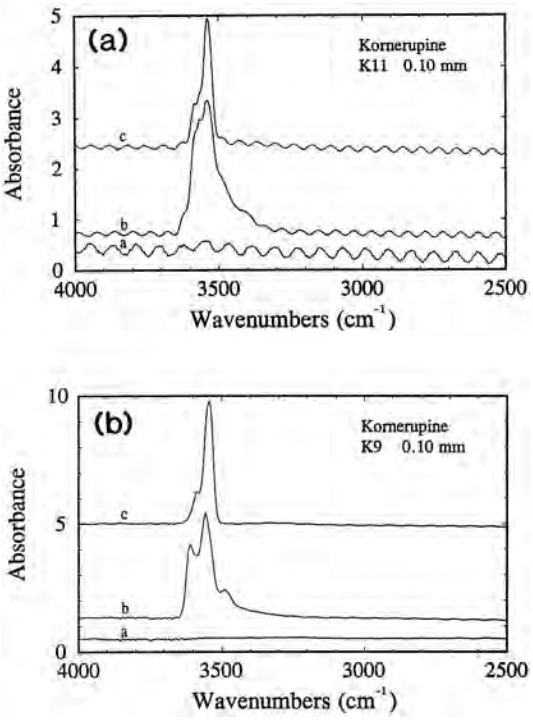

FIG. 10. Polarized infrared spectra of crystals (a) K11 and (b) K9; the direction of the electric vector is shown by the lower-case letter (a, b or c) at the left of each spectrum.

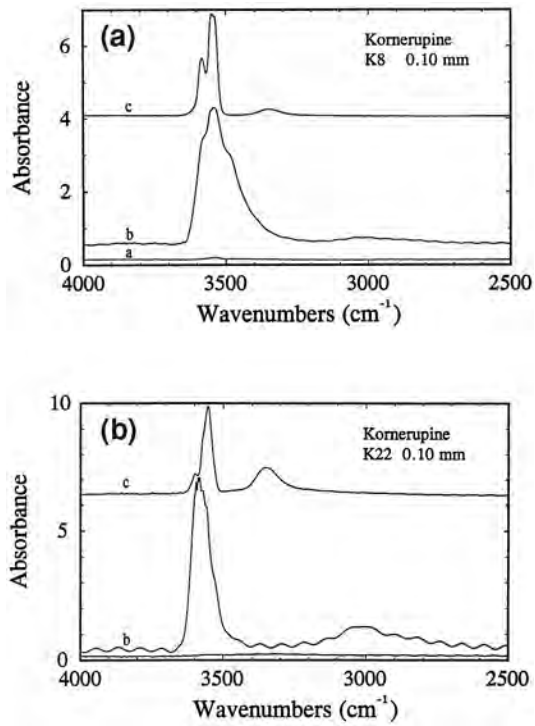

FIG. 11. Polarized infrared spectra of crystals (a) K8 and (b) K22; legend as in Figure 10.

[*i.e.*, *H*(1)], then the O–H bond is parallel to the *b* axis of the crystal; for the E || *b* spectrum, the electric vector is parallel to the O–H bond, and a strong absorption occurs in this direction, whereas for the E || *c* spectrum, there is no (non-zero) component of the electric vector parallel to the O–H bond, and hence there is no absorption. If the H atom occupies the Wyckoff position 8*f* [*i.e.*, *H*(2)], the O–H bond lies off the mirror plane at $z = ¼$ at (non-zero and non-orthogonal) angles to the *b* and *c* axes; for both E || *b* and E || *c* spectra, non-zero components of the electric vector are parallel to the O–H bond, and absorptions result in both spectra.

Short-range order and local bond-valence considerations

In order to assign the bands in the spectra of Figures 10 and 11, we need to consider the short-range (local) arrangements around the *H* sites, as these will affect the strength of the hydrogen bonds formed and hence the frequencies of their absorptions. In addition to the *H* sites, the O(10) site is coordinated by two *M*(1) sites and two *X* sites, and the O(9) site is coordinated by two *T*(1) sites and two *X* sites. The *X* site is occupied by 0.7 □ + 0.3 M^{2+} on average, and because of the close approach of the *H* sites to the *X* site, the *X* and *H* sites cannot be locally occupied simultaneously. Thus where one *X* site is occupied in a local configuration, the adjacent *H*(2) site is vacant; similarly, where one *H*(2) site is occupied in a local configuration, the adjacent *X* site is vacant. Similarly, where an *H*(1) site is occupied, the two adjacent *X* sites must be vacant. The *T*(1) site can be occupied by Si or Al, and hence the O(9) anion can be coordinated by two $^{T(1)}$Si atoms or by $^{T(1)}$Si + $^{T(1)}$Al; the Al occupancy of the *T*(1) site is sufficiently low that coordination by two $^{T(1)}$Al will not occur. As the *H*(1)...O(9) distance (1.80–1.90 Å) is less than the *H*(2)...O(9) distance (>2.21 Å), the bond valence of *H*(1)...O(9) will be larger than that of *H*(2)...O(9). The *T*(1)*T*(1) arrangement AlSi will supply less bond-valence to O(9) than the SiSi arrangement. Hence to satisfy the *local* bond-valence requirements of the O(9) anion, the *H*(2)...O(9) interaction must combine with the Si–O(9)–Si arrangement, and the *H*(1)...O(9) interaction must combine with the Si–O(9)–Al arrangement. Thus we may identify the three local arrangements shown in Figure 12 as occurring around the O(9) and O(10) sites in kornerupine, and we may use the shorthand notation indicated to denote each configuration: [X□, SiSi, *H*(2)]; [□□, SiSi, *H*(2)]; [□□, SiAl, *H*(1)].

Assignment of bands

Configurations [X□, SiSi, *H*(2)] and [□□, SiSi, *H*(2)] will have absorption bands in both the E || *b* and E || *c* spectra, whereas configuration [□□, SiAl, *H*(1)] will have an absorption band only in the E || *b* spectrum. The principal stretching frequency of the (OH) bond is inversely related to the length (≡ bond valence) of the H…O hydrogen bond, and we can assign the bands

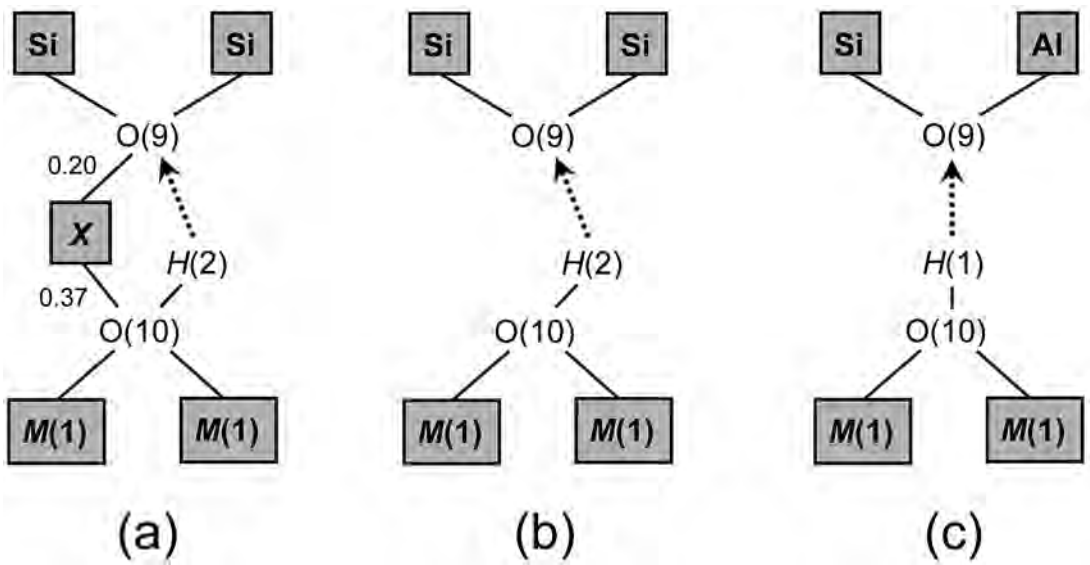

FIG. 12. Short-range configurations around the O(9) and O(10) sites in kornerupine: (a) *X* site occupied, *H*(2) site occupied; (b) *X* site vacant, *H*(2) site occupied; (c) *X* site and *H*(2) site both vacant, *H*(1) site occupied. Hydrogen bonds are shown as dotted lines, and the bond valences of the *X*–O(9) and *X*–O(10) bonds are shown (in *vu*) in (a).

using this criterion, combined with the polarization characteristics of the bands.

Where the *X* site is occupied, the average bond-valence from the *X* cation to O(9) and O(10) is 0.20 and 0.37 *vu*, respectively (Fig. 12a). Therefore, in the absence of the *X* cation (Fig. 12b), the bond-valence deficit is greater at O(10) than at O(9), and the bond-valence requirements for the O atom at O(10) are met *via* shortening of the O(10)–*M*(1) and O(10)–*H*(2) bonds. This, in turn, results in a relatively weaker *H*(2)...O(9) bond for the [□□, SiSi, *H*(2)] configuration, and the remaining bond-valence requirements for the O atom at O(9) are met *via* shortening of the *T*(1)–O(9) bond. The resultant band for the [□□, SiSi, *H*(2)] configuration (Band A; Figs. 10 and 11, Table 2) will therefore be displaced to a higher frequency than the band for the [X□, SiSi, *H*(2)] configuration (band B). The straight hydrogen bond [*H*(1)...O(9)] that is involved in the [□□, SiAl, *H*(1)] configuration is much shorter (1.80–1.90 Å) and provides greater bond-valence to O(9) in order to offset the significant bond-valence deficiency associated with the presence of SiAl at the *T*(1)–*T*(1) dimer. Hence, the band from the [□□, SiAl, *H*(1)] configuration (band D) will occur at a lower frequency than either bands A and B that are associated with the longer (bent) O(10)–*H*(2)...O(9) arrangement.

This leaves the C and E bands still unassigned. As shown in Figure 13, there is a strong correlation between the intensities of the C and E bands, suggesting that they have the same origin. However, the C band is polarized E ∥ *c* and the E band is polarized E ∥ *b*, and hence these bands cannot be due to a configuration involving a H atom. The C band is too sharp to be a low-lying crystal-field band involving Fe^{2+}; the origin of the C and E bands is unknown.

Careful inspection of the band envelopes show that some of the spectra (*e.g.*, K11) show additional shoulders on the main A and B absorptions (Fig. 10a). Sample K11 contains the most Fe of the samples studied (^{X}Fe = 0.13, ^{X}Mg = 0.07, $^{M(1)}$Fe = 0.71, $^{M(1)}$Mg = 1.29 *pfu*) (Cooper *et al.* 2009), and this fine structure in the spectra is due to Mg ⇌ Fe^{2+} substitution at the sites [*X*, *M*(1)] coordinating the O(10) anion; however, the resolution is not sufficient to derive any quantitative information about short-range order.

Band Intensity and the Occupancy of the *X* Site

As the A, B and D bands are assigned to configurations (b), (a) and (c) (Fig. 12), the relative intensity of the B and A + D bands must be related to the degree of occupancy of the *X* site. This issue is somewhat complicated by the fact that adjacent *X* sites cannot

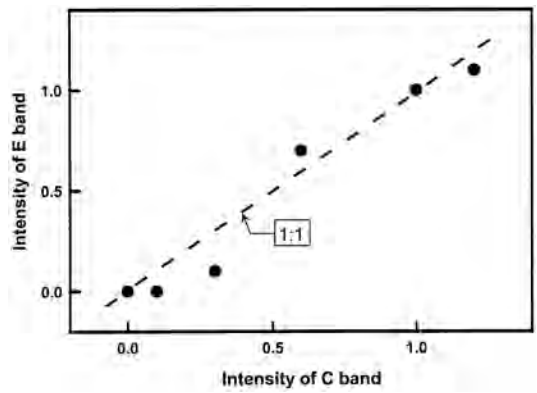

FIG. 13. Correlation between the intensities of the E band and the C band in the infrared spectra of kornerupine–prismatine crystals. The dashed line has a slope of 1.

TABLE 2. POSITIONS (cm^{-1}) AND INTENSITIES* (a.u.) OF ABSORPTION BANDS IN THE INFRARED FOR SELECTED CRYSTALS OF KORNERUPINE–PRISMATINE

	E ∥ *c*						E ∥ *b*							
	A		B		C		A		B		D		E	
K1	3574	w	3544	4.2	3350	1.0(b)	<3563>	–	<3563>	–	3482	w	3014	1.0(b)
K6	3581	1.3	3541	4.6	–	–	3581	s	3541	3.7	3491	2.4	–	–
K8	3585	1.5	3545	2.8	3352	0.2(b)	3586	2.8	3541	3.7	3484	2.4	–	–
K9	3585	1.2	3544	4.6	–	–	3610	2.8	3555	4	3484	1	–	–
K11	3581	0.9	3540	2.3	–	–	3580	2.1	3542	2.6	3484	1	–	–
K13	3600	2.3	3556	4	–	–	3607	4.5	3556	3.6	3480	0.2	–	–
K15	3579	1	3540	3.6	3313	0.1(b)	3591	2.3	3540	3.1	3489	1.5	–	–
K22	3600	0.9	3553	3.3	3349	0.6(b)	<3575>	–	<3575>	–	–	–	3011	0.7(b)
K23	3587	1.3	3556	4	3326	0.3(b)	<3596>	–	3556	3.9	–	–	3017	0.1(b)
K24	3584	0.9	3536	2.5	–	–	3617	1.4	3570	3.1	3486	1.3	–	–

vs: very strong; s: strong; w: weak; b: broad; a.u.: absorbance units. * Where peak positions are given in < >, the band has gone off the intensity scale.

be occupied (Fig. 9a), and hence local coupling plays an important role in this respect. Configuration [X□, SiSi, *H*(2)] (Fig. 12a) is associated with arrangements of type (b) in Figure 7 and gives rise to band B (Table 2), whereas configurations [□□, SiSi, *H*(2)] (Fig. 12b) and [□□, SiAl, *H*(1)] (Fig. 12c) are associated with arrangements of type (a) in Figure 7 and gives rise to bands A and D (Table 2). Arrangements (a) and (b) (Fig. 7) are end-member situations in the kornerupine structure: only (a) will result in zero occupancy of *X*, and only (b) will allow for up to half occupancy of *X* (the maximum possible occupancy of this site). The occupancy of the *X* site varies from 0.21 to 0.36 in the crystals examined spectroscopically, indicating that the arrangements (a) and (b) (Fig. 7) will occur in the ranges 0.58 to 0.28 and 0.42 to 0.72, respectively [assuming maximal *X*-site occupancy for arrangement (b)]. We cannot quantitatively relate the relative intensities of the A, B and D bands to the occupancies of the *X* site because the angle O(10)–*H*(2)...O(9) varies significantly even in a single crystal (Fig. 4). However, the relative intensities of the B and A + D bands are in reasonable accord with the range of *X*-site occupancies in the crystals examined.

Conclusions

(1) The (OH + F) content of kornerupine is 1.0 *apfu*; there is no (H_2O) or O^{2-} at this site.

(2) The maximum possible occupancy of the *X* site is (1 + F)/2.

(3) Polarized infrared spectra in the principal (OH)-stretching region show fine structure that can be assigned to specific short-range arrangements of cations around the O(10) site.

(4) There is strong short-range order around the O(9) and O(10) sites, connected with local occupancy of the *X* sites by divalent cations and vacancies, occupancy of the adjacent pair of *T*(1) sites by Si–Si or Si–Al, occupancy of the adjacent *M*(1) sites by Mg or Fe^{2+}, and occupancy of the *H*(1) or *H*(2) sites by H.

Acknowledgements

We thank Gianni Andreozzi, Sergio Lucchesi and Ron Peterson for their perspicacious comments on this paper. We thank Kurt Kyser for the HLE measurements. Financial support was provided by Natural Sciences and Engineering Research Council of Canada in the form of a Canada Research Chair to FCH, Discovery and Equipment Grants to FCH, and by NSF (USA) grants EAR–9405438 and EAR–0337816 to GRR.

References

Cooper, M.A., Hawthorne, F.C. & Grew, E.S. (2009): The crystal chemistry of the kornerupine–prismatine series. I. Crystal structure and site populations. *Can. Mineral.* **47**, 233-262.

Finger, L.W. & Hazen, R.M. (1981): Refinement of the crystal structure of an iron-rich kornerupine. *Carnegie Inst. Wash., Year Book* **80**, 370-373.

Grew, E.S. (1996): Borosilicates (exclusive of tourmaline) and boron in rock-forming minerals in metamorphic environments. *In* Boron: Mineralogy, Petrology and Geochemistry (E.S. Grew & L.M. Anovitz, eds.). *Rev. Mineral.* **33**, 387-502.

Hawthorne, F.C. (1995): Light lithophile elements in metamorphic rock-forming minerals. *Eur. J. Mineral.* **7**, 607-622.

Hawthorne, F.C., Groat, L.A., Raudsepp, M. & Ercit, T.S. (1987): Kieserite, $Mg(SO_4)(H_2O)$, a titanite-group mineral. *Neues Jahrb. Mineral., Abh.* **157**, 121-132.

Klaska, R. & Grew, E.S. (1991): The crystal structure of B-free kornerupine: conditions favoring the incorporation of variable amounts of B through $^{[4]}B \leftrightarrow {}^{[4]}Si$ substitution in kornerupine. *Am. Mineral.* **76**, 1824-1835.

Kyser, T.K. & O'Neil, J.R. (1984): Hydrogen isotope systematics of submarine basalts. *Geochim. Cosmochim. Acta* **48**, 2123-2133.

Moore, P.B. & Araki, T. (1979): Kornerupine: a detailed crystal-chemical study. *Neues Jahrb. Mineral., Abh.* **134**, 317-336.

Moore, P.B. & Bennett, J.M. (1968): Kornerupine: its crystal structure. *Science* **159**, 524-526.

Moore, P.B., Sen Gupta, P.K. & Schlemper, E.O. (1989): Kornerupine: chemical crystallography, comparative crystallography, and its cation relation to olivine and to Ni_2In intermetallic. *Am. Mineral.* **74**, 642-655.

Ottolini, L., Cámara, F. & Hawthorne, F.C. (2002): Quantification of H, B and F in kornerupine: accuracy of SIMS and SREF (X-ray single-crystal structure refinement) data. *Mikrochim. Acta* **139**, 125-129.

Received March 16, 2006, revised manuscript accepted March 27, 2009.